

Size-dependent melting properties of Sn nanoparticles by chemical reduction synthesis

ZOU Chang-dong(邹长东), GAO Yu-lai(高玉来), YANG Bin(杨斌), ZHAI Qi-jie(翟启杰)

Shanghai Key Laboratory of Modern Metallurgy and Materials Processing,
Shanghai University, Shanghai 200072, China

Received 5 December 2008; accepted 4 January 2009

Abstract: Tin nanoparticles with different size distribution were synthesized using chemical reduction method by applying NaBH_4 as reduction agent. The Sn nanoparticles smaller than 100 nm were less agglomerated and no obviously oxidized. The melting properties of these synthesized nanoparticles were studied by differential scanning calorimetry. The melting temperatures of Sn nanoparticles in diameter of 81, 40, 36 and 34 nm were 226.1, 221.8, 221.1 and 219.5 °C, respectively. The size-dependent melting temperature and size-dependent latent heat of fusion have been observed. The size-dependent melting properties of tin nanoparticles in this study were also comparatively analyzed by employing different size-dependent theoretical melting models and the differences between these models were discussed. The results show that the experimental data are in accordance with the LSM model and SPI model, and the LSM model gives the better understanding for the melting property of the Sn nanoparticles.

Key words: Sn nanoparticle; chemical reduction; melting; size-dependent property

1 Introduction

Tin is an essential element used for the electronic interconnect materials in electronic devices. Sn-Pb alloy is a traditional material which has been used for interconnect materials for a long history. However, due to the inherent toxicity and the harm to human health and environment, Sn-Pb alloy is gradually being phased out of the electronic industry in more and more countries. Some Sn-based lead-free interconnect materials have been developed with the inherent disadvantages of higher melting temperature than Sn-Pb eutectic alloy. The high melting temperature of these lead-free alloys will cause some adverse effects such as energy consumption and substrate warpage, resulting in relatively poor reliability of the electronic devices. In this case, the research on lowering the melting temperature of Sn and Sn-based lead-free interconnect materials is being paid attention.

The melting temperature of pure metals can be decreased by reducing their size to nanometer scale, showing size-dependent properties. After the first observation of the melting temperature depression for nanosized thin metal films of Sn, Bi and Pb reported by

TAKAGI[1], the size-dependent melting properties of lots of pure metals, such as Sn[2], Ag[3], Cu[4], Al[5], In[6], Pb[7], Au[8] and Bi[9], have been studied both on theory and experiment. The melting temperature depression is caused by the high ratio of surface area to volume for small particles. The in-situ transmission electron microscope (TEM)[10–11] and nanocalorimeter [2, 12] have been used for studying the melting behaviors of Sn nanoparticles. However, the disadvantage of in-situ TEM is that it can only be used to measure the pre-melting temperature, which is different from the normal melting temperature. LAI et al[12] used nanocalorimeter for studying the melting properties of Sn nanoparticles and reported the size-dependent properties of the latent heat of fusion of Sn nanoparticles for the first time. However, as for both TEM and nanocalorimeter measurements, the Sn nanoparticles or clusters were prepared directly in the measurement equipment in order to prevent the oxidation of the sample. As mentioned above, it is necessary to obtain independent particles to lower the melting temperature of Sn and Sn-based lead-free interconnect materials. So, for the in-service application in the electronic industry, the synthesis and characterization of independent particles

Foundation item: Project(2006AA03Z339) supported by the National High-tech Research and Development Program of China; Project(50571057) supported by the National Natural Science Foundation of China; Project(08520740500) supported by Science and Technology Commission of Shanghai Municipality, China

Corresponding author: GAO Yu-lai; Tel: +86-21-56332144; E-mail: gaoyulai@163.com
DOI: 10.1016/S1003-6326(09)60130-8

should be emphasized. JIANG et al[13–14] have reported the attempt for lowering the melting temperature of the Sn and Sn-Ag lead free solder. In the present study, Sn nanoparticles with less oxidation were prepared and their size-dependent melting properties were systematically discussed.

2 Experimental

Tin (II) 2-ethylhexanoate ($C_{16}H_{30}O_4Sn$), sodium borohydride ($NaBH_4$), 1,10-phenanthroline ($C_{12}H_8N_2 \cdot H_2O$) and anhydrous methanol (CH_3OH) were used as precursor, reducing agent, surfactant and solvent, respectively.

In a typical synthesis process, 0.33 g of tin (II) 2-ethylhexanoate and 0.1 g of 1, 10-phenanthroline were mixed in 60 mL anhydrous methanol solution. The solution was then mechanically stirred intensively for 2 h. Then, 0.2 g of sodium borohydride was added to the solution and the reaction continued for another 2 h at room temperature. In different cases, different amounts of surfactant, 0, 0.1, 0.2, and 0.4 g, were chosen to control the morphology and size distribution of the products. After the reaction completed, the obtained products were centrifugally separated at 4 000 r/min for 45 min and rinsed several times with a large amount of absolute ethanol, and finally dried in vacuum at 60 °C for 4 h.

The products were characterized by means of X-ray diffraction from 20° to 90° on a Rigaku D/Max–2200 X-ray diffractometer. The FE-SEM (JSM–6700F) was used to observe morphology of the as-prepared nanoparticles. SEM specimens were prepared by dispersing a few drops of the Sn nanoparticles solution on silicon substrate. The melting temperature of Sn nanoparticles was measured by differential scanning calorimeter (DSC, TA Instruments, model SDT–Q600). The Sn nanoparticles were dispersed in ethanol by means of ultrasonic vibration, and then dropped into the Al_2O_3 crucible and placed in the DSC cell. The samples were heated at heating rate of 10 °C/min from room temperature to 300 °C, and then cooled down at the same rate, with the protection of high-purity nitrogen.

3 Results and discussion

On the basis of the aforementioned chemical reduction process, Sn nanoparticles could be prepared. Fig.1 shows the XRD patterns of the as-synthesized Sn nanoparticles. All the four XRD patterns could be readily indexed to the tetragonal phase of Sn (space group $I41/$ and (141), lattice constants $a=0.583$ 1 nm and $c=0.318$ 2 nm (JCPDS 04-0673)). The relative intensity of the

peaks was consistent with that of the Sn nanoparticles reported elsewhere[13]. From the XRD patterns, no obvious oxidation peaks were found, even though no surfactant was applied during the synthesis process (see Fig.1(a)). This result was different from that reported in Ref.[13], in which oxidation traces of SnO_2 were clearly observed from the XRD pattern of the Sn nanoparticles synthesized without the presence of surfactant.

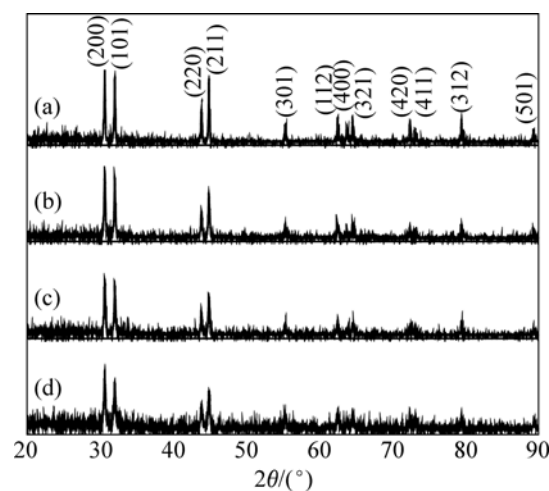


Fig.1 XRD patterns of Sn nanoparticles synthesized by using 0.33 g of tin (II) 2-ethylhexanoate as precursor in the presence of different amounts of surfactant: (a) 0 g; (b) 0.1 g; (c) 0.2 g; (d) 0.4 g

The morphology of the as-synthesized Sn nanoparticles was observed by FE-SEM. Fig.2 shows the typical SEM images of Sn nanoparticles synthesized by using 0.33 g of tin (II) 2-ethylhexanoate as precursor in the presence of different amounts of surfactant. It was found that the larger the mass ratio of the surfactant to the precursor, the smaller the particle size. This is due to the capping effect caused by the surfactant molecules coordinate with the nanoclusters, and resultantly a larger amount of surfactant restricts the growth of Sn nanoparticles[13].

Fig.3 shows the determination of particle size distribution of the four kinds of Sn nanoparticles. The data were fitted with a Gaussian model, and the average particle diameters were around 82 nm, 39 nm, 36 nm, and 34 nm, respectively.

Fig.4 shows the DSC curves of the as-synthesized Sn nanoparticles. The Sn nanoparticles synthesized using 0.33 g of tin (II) 2-ethylhexanoate as precursor in the presence of 0, 0.1, 0.2 and 0.4 g surfactants were marked as Sn1, Sn2, Sn3 and Sn4, respectively. The melting temperatures of the Sn1, Sn2, Sn3 and Sn4 nanoparticles were 226.1, 221.8, 221.1 and 219.5 °C, and the corresponding latent heats of fusion were 35.9, 23.5, 20.1 and 15.6 J/g, respectively. The detailed results obtained from the DSC curves are listed in Table 1.

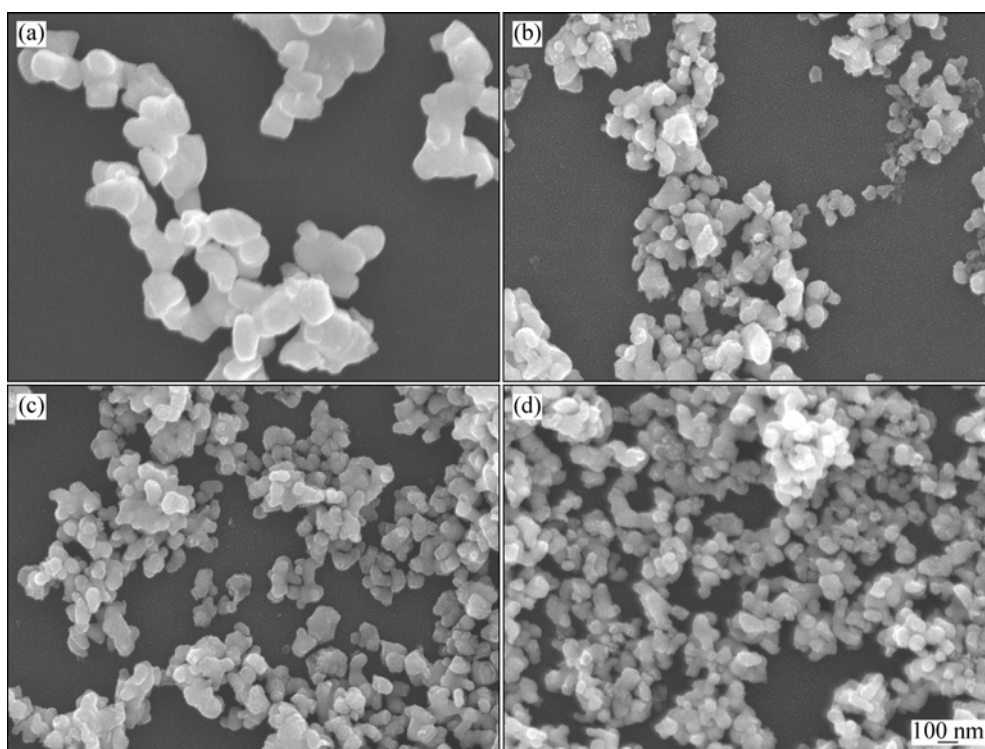


Fig.2 SEM images of Sn nanoparticles synthesized by using 0.33 g of tin (II) 2-ethylhexanoate as precursor in the presence of different amounts of surfactant: (a) 0 g; (b) 0.1 g; (c) 0.2 g; (d) 0.4 g

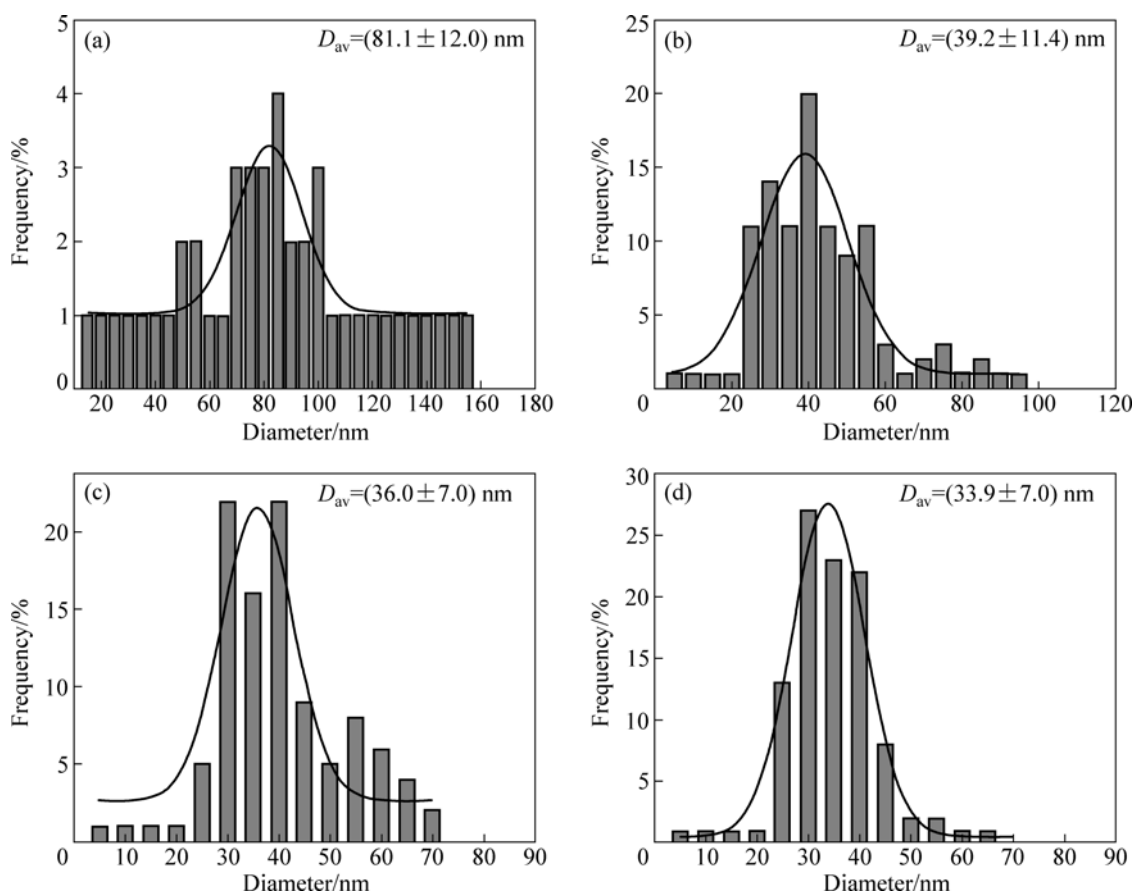


Fig.3 Particle diameter histograms of Sn nanoparticles synthesized by using 0.33 g of tin (II) 2-ethylhexanoate as precursor in the presence of different amounts of surfactant: (a) 0 g; (b) 0.1 g; (c) 0.2 g; (d) 0.4 g

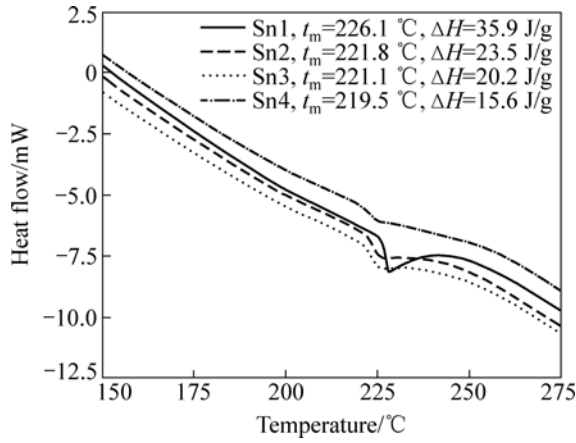


Fig.4 DSC curves of four kinds of synthesized Sn nanoparticles

Table 1 Melting temperatures and latent heats of fusion of Sn nanoparticles obtained from DSC measurements

Sample	Diameter/nm	$t_m/^\circ\text{C}$	$\Delta t_m/^\circ\text{C}$	$\Delta H/(\text{J}\cdot\text{g}^{-1})$
Sn bulk[12]		232.0	–	58.9
Sn1	82.1 ± 12.0	226.1	5.9	35.9
Sn2	39.2 ± 11.4	221.8	10.2	23.5
Sn3	36.0 ± 7.0	221.1	10.9	20.2
Sn4	33.9 ± 7.0	219.5	11.5	15.6

By considering the existed surface melting of the particle as the solid particle is coated with a thin liquid layer prior to melting, WRONSKI[10] obtained the liquid-skin melting model (LSM model) for Sn nanoparticles. The melting temperature of the particle is taken as the equilibrium temperature of the solid sphere core with the liquid shell of a given critical thickness h_0 , where h_0 is an adjustable parameter in accordance with the experimental results. Accordingly, the melting point t_m of Sn nanoparticles with diameter(d) is expressed as follows[10]:

$$t_0 - t_m = \frac{4t_0}{\Delta H_0} \left\{ \frac{\sigma_{sl}}{\rho_s(d-2h_0)} + \frac{\sigma_{lv}}{d} \left[\frac{1}{\rho_s} - \frac{1}{\rho_l} \right] \right\} \quad (1)$$

where t_0 is the melting temperature of bulk Sn; ΔH_0 is the latent heat of fusion; σ_{sl} and σ_{lv} are the interfacial surface tensions between solid and liquid, and between liquid and vapor, respectively; ρ_s and ρ_l are the densities of the solid and the liquid; d is the diameter of the particle; and h_0 is the critical thickness of the liquid layer at t_m .

Substituting $t_0=232^\circ\text{C}$, $\rho_s=7.18\text{ g/cm}^3$, $\rho_l=6.98\text{ g/cm}^3$, and $\sigma_{lv}=550\text{ mN/m}$ into Eq.(1), the following equation can be obtained[12]:

$$t_m = 232 - 156.4 \left[\frac{\sigma_{sl}}{15.8(d-2h_0)} - \frac{1}{d} \right] \quad (2)$$

where σ_{sl} was determined to be $(48 \pm 8)\text{ mN/m}$ [12].

By adjusting the value of the critical liquid layer thickness, a best fit to the experimental data in terms in Eq.(2) of $h_0=(2.87 \pm 0.53)\text{ nm}$ was obtained (see Fig.5).

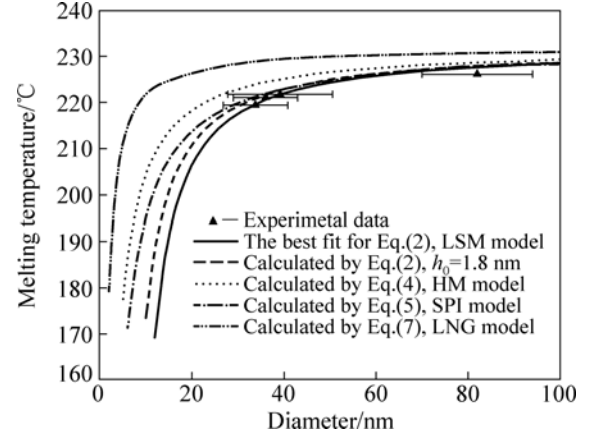


Fig.5 Size-dependent melting temperature of Sn nanoparticle

BUFFAT and BOREL[15] obtained the homogeneous melting model (HM model) for small particles, assuming that the solid and liquid particles with the same mass are in equilibrium with their common vapor. The HM model can be expressed by the following equation:

$$t_m = t_0 \left\{ 1 - \frac{4}{\rho_s \Delta H_0 d} \left[\sigma_{sv} - \sigma_{lv} \left(\frac{\rho_s}{\rho_l} \right)^{2/3} \right] \right\} \quad (3)$$

where σ_{sv} is the interfacial surface tension between the solid and its vapor.

Substituting $\rho_s=7.18\text{ g/cm}^3$, $\rho_l=6.98\text{ g/cm}^3$, $\sigma_{lv}=550\text{ mN/m}$ and $\sigma_{sv}=685\text{ mN/m}$ [16] into Eq.(3), we obtained the following equation:

$$t_m = t_0 \left(1 - \frac{1.178}{d} \right) \quad (4)$$

By using the surface-phonon interaction theory, WAUTELET[17] obtained the surface-phonon instability melting model (SPI model), which can be expressed as follows:

$$t_m = t_0 \left(1 - \frac{\beta}{d} \right) \quad (5)$$

where β is a constant, 1.57 for Sn nanoparticles[17].

Treating the melting of small particles as a liquid nucleation and growth (LNG model) process, COUCHMAN and JESSER[18] obtained the LNG size-dependent melting model for small particles. At the melting temperature, a liquid layer with thickness δ is formed on the surface and σ moves at a substantial rate into the solid, then the LNG model can be expressed as follows[18]:

$$t_m = t_0 \left[1 - \frac{4\sigma_{sl}}{\rho_s \Delta H_0 (d - 2\delta)} \right] \quad (6)$$

Normally, δ is very small compared with r , and thereby the upper limit of the melting temperature derived by LNG model can be expressed as follows[18]:

$$t_m = t_0 \left[1 - \frac{4\sigma_{sl}}{\rho_s \Delta H_0 d} \right] \quad (7)$$

Fig.5 shows the size-dependent melting of tin nanoparticles. The lines were calculated by the above mentioned four size-dependent melting models. The dashed line was calculated by LSM model with $h_0=1.8$ nm which was obtained by LAI et al[12]. The solid line is a best fit for the LSM model, with a best fit of $h_0 = 2.87$ nm, which is reasonably consistent with the value obtained by LAI et al[12]. The dash dotted line was calculated by SPI model. It can be seen that the experimental data are also in reasonable agreement with the SPI model. The dotted line is calculated by HM model. The dash dot dotted line is the upper limit of the melting temperature which was calculated by LNG model, showing that our experimental data are all lower than the calculated upper limits. Considering the size error, our experimental data are in reasonable agreement with LSM model and SPI model.

It is found that Eq.(6) and Eq.(1) are similar if volume difference between solid and liquid is neglected. However, the LNG model is essentially different from the LSM model. In LNG model, an unstable surface liquid layer is formed which stands for an unstable equilibrium state of the system, and melting occurs as the energy barrier is overcome by thermal fluctuations of the system. As to LSM model, surface melts prior to the solid cores, i.e. the liquid skin exists in prior and are in stable equilibrium with the core below the melting temperature[19]. The upper limits of the melting temperature can be obtained by LNG model. The LSM model gives a better understanding of the size-dependent property of Sn nanoparticles. The formation of a molten surface overlayer equilibrated with the solid core is directly related to the surface melting phenomenon which has been observed by many researchers by in-situ TEM. For example, TAKAGI[1] observed the surface melting phenomena of Sn, Bi, and Pb thin films by TEM for the first time in 1954. The surface melting of Pb small particles was also detected by X-ray diffraction, and the liquid skin thickness on 50 nm crystallites was determined to be 0.5 nm by calculating from the intensity and the peak shape of the diffraction peaks, showing adequate evidence for the LSM size-dependent melting model[7, 20]. For SPI model, the surface of the small

particles is treated to be similar to the defects. The concentration of the defects is proportional to the ratio of the number of surface atoms and the total number of atoms in the small particles[17]. In this case, the surface atoms play an important role in the melting of the small particles. From Fig.5, it is clear that the experimental results are also in agreement with the SPI model.

The size-dependent property of the latent heat of fusion of the Sn nanoparticles is also observed (See Table 1). The size-dependent property of the latent heat of fusion of the Sn nanoparticles has also been reported elsewhere[12, 21]. LAI et al[12] obtained the following expression for the size-dependent latent heat of fusion for Sn nanoparticles in terms of the particle diameter:

$$\Delta H_m = \Delta H_0 \left(1 - \frac{2h_0}{d} \right)^3 \quad (8)$$

where ΔH_m is the latent heat of fusion for Sn nanoparticles; ΔH_0 is the latent heat of fusion for bulk Sn; and h_0 is the thickness of the surface melting layer.

In LAVCEVIC and OGORLEC'S research[21], the latent heat of fusion of the aggregates of Sn nanoparticles seems to follow a simple dependence on the average particle diameter d :

$$\Delta H_m \propto d \quad (9)$$

In this work, the latent heat of fusion for the Sn nanoparticles seems to follow another dependence on the average particle diameter as the following expression:

$$\left(\frac{\Delta H_m}{\Delta H_0} \right)^{(1/3)} \propto d \quad (10)$$

Fig.6 shows the size-dependent properties of latent heat of fusion for the Sn nanoparticles obtained in this work. By linear fit of the experimental data, the latent heat of fusion of Sn nanoparticles can be expressed as follows:

$$\left(\frac{\Delta H_m}{\Delta H_0} \right)^{(1/3)} = 0.98 - \frac{10.62}{d} \quad (11)$$

In light of Eq.(11), when $d=\infty$, which stands for the bulk Sn, the value of latent heat of fusion ΔH_m is 55.4 J/g, lower than ΔH_0 . Considering the light oxidation during the DSC scanning, the result obtained in this work is acceptable. When the latent heat of fusion, $\Delta H_m=0$, the critical value of the particle diameter is 5.4 nm, which is in accordance with the value obtained by LAVCEVIC and OGORLEC[21]. In their report, the latent heat of fusion would disappear for the particles of critical size of around 5 nm, and the sample with average diameter of 2.7 nm showed no phase transition effects.

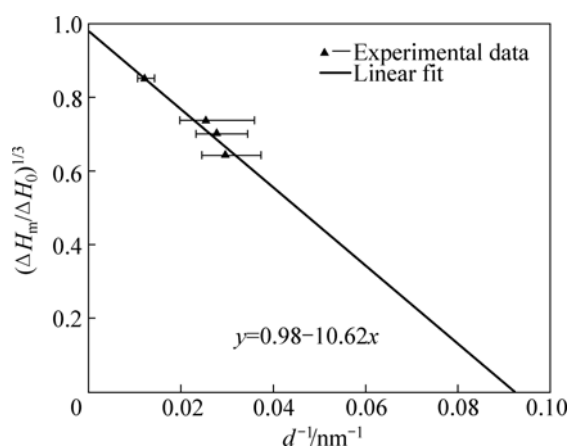


Fig.6 Size-dependent latent heat of fusion of Sn nanoparticles

4 Conclusions

1) Tin nanoparticles with different size distributions were successfully synthesized by chemical reduction method with different amounts of surfactant, which were also used to prevent the synthesized Sn nanoparticles from aggregation and oxidation. Both size-dependent properties of melting temperature and latent heat of fusion were observed from the DSC results.

2) Different size-dependent melting models (LSM, SPI, LNG and HM) were comparatively used to analyze the size-dependent melting temperatures properties of the synthesized Sn nanoparticles. The results show that the experimental data are in accordance with the LSM model and SPI model, and the LSM model gives the better understanding for the melting property of the Sn nanoparticles. All the experimental data are lower than the upper limits of the melting temperatures calculated from the LNG model.

3) The latent heat of fusion of the Sn nanoparticles was also analyzed, and the results show that the cube root of the latent heat of fusion of Sn nanoparticles is linearly dependent on the reciprocal of the average particle diameter. According to these models, the surface of the small particles plays an important role in its melting properties.

References

[1] TAKAGI M. Electron-diffraction study of liquid-solid transition of thin metal films [J]. *Journal of the Physical Society of Japan*, 1954, 9(3): 359–363.

- [2] BACHELS T, GUTHERODT H J, SCHAER R. Melting of isolated tin nanoparticles [J]. *Physical Review Letters*, 2000, 85(6): 1250–1253.
- [3] QUAAS M, SHYJUMON I, HIPPLER R, WULFF H. Melting of small silver clusters investigated by HT-GIXRD [J]. *Zeitschrift für Kristallographie*, 2007, 26(S): 267–272.
- [4] WANG L, ZHANG Y, BIAN X, CHEN Y. Melting of Cu nanoclusters by molecular dynamics simulation [J]. *Physics Letters A*, 2003, 310: 197–202.
- [5] SUN J, SIMON S L. The melting behavior of aluminum nanoparticles [J]. *Thermochimica Acta*, 2007, 463(1/2): 32–40.
- [6] DIPPPEL M, MAIER A, GIMPLE V, WIDER H, EVENSON W E, RASERA R L, SCHATZ G. Size-dependent melting of self-assembled indium nanostructures [J]. *Physical Review Letters*, 2001, 87(9): 095505.
- [7] PETERS K F, COHEN J B, CHUNG Y W. Melting of Pb nanocrystals [J]. *Physical Review B*, 1998, 57(21): 13430.
- [8] WANG Y, TEITEL S, DELLAGO C. Melting and equilibrium shape of icosahedral gold nanoparticles [J]. *Chemical Physics Letters*, 2004, 394(4/6): 257–261.
- [9] OLSON E A, EFREMOV M Y, ZHANG M, ZHANG Z, ALLEN L H. Size-dependent melting of Bi nanoparticles [J]. *Journal of Applied Physics*, 2005, 97(3): 034304–034309.
- [10] WRONSKI C R M. The size dependence of the melting point of small particles of tin [J]. *British Journal of Applied Physics*, 1967, 18(12): 1731–1737.
- [11] ALLEN G L, BAYLES R A, GILE W W, JESSER W A. Small particle melting of pure metals [J]. *Thin Solid Films*, 1986, 144(2): 297–308.
- [12] LAI S L, GUO J Y, PETROVA V, RAMANATH G, ALLEN L H. Size-dependent melting properties of small tin particles: Nanocalorimetric measurements [J]. *Physical Review Letters*, 1996, 77(1): 99.
- [13] JIANG H, MOON K S, DONG H, HUA F, WONG C P. Size-dependent melting properties of tin nanoparticles [J]. *Chemical Physics Letters*, 2006, 429(4/6): 492–496.
- [14] JIANG H, MOON K S, HUA F, WONG C P. Synthesis and thermal and wetting properties of tin/silver alloy nanoparticles for low melting point lead-free solders [J]. *Chemistry of Materials*, 2007, 19(18): 4482–4485.
- [15] BUFFAT P, BOREL J P. Size effect on the melting temperature of gold particles [J]. *Physical Review A*, 1976, 13(6): 2287.
- [16] JESSER W A, SHIFLET G J, ALLEN G L, CRAWFORD J L. Equilibrium phase diagrams of isolated nano-phases [J]. *Materials Research Innovations*, 1999, 2(4): 211–216.
- [17] WAUTELET M. Estimation of the variation of the melting temperature with the size of small particles, on the basis of a surface-phonon instability model [J]. *Journal of Physics D: Applied Physics*, 1991, 24(3): 343–346.
- [18] COUCHMAN P R, JESSER W A. Thermodynamic theory of size dependence of melting temperature in metals [J]. *Nature*, 1977, 269(5628): 481–483.
- [19] MEI Q S, LU K. Melting and superheating of crystalline solids: From bulk to nanocrystals [J]. *Progress in Materials Science*, 2007, 52(8): 1175–1262.
- [20] KEVIN F P, YIP-WAH C, JEROME B C. Surface melting on small particles [J]. *Applied Physics Letters*, 1997, 71(16): 2391–2393.
- [21] LAVCEVIC M L, OGORELEC Z. Melting and solidification of Sn-clusters [J]. *Materials Letters*, 2003, 57(26/27): 4134–4139.

(Edited by YANG Hua)